RESEARCH ARTICLE

A CAE-Based Methodology for Designing a Fuel Cell Stack for Electric Vehicle Applications

Sanketh Ramachandra[1], Anindya Deb[1*], Purushothama Chippar[2]

[1]*Centre for Product Design and Manufacturing, Indian Institute of Science, Bangalore, Karnataka, 560012, India*

[2] *Department of Mechanical Engineering, St. Joseph Engineering College, Mangalore, India*

ABSTRACT: Battery powered electric vehicles which can be considered as affordable for a common buyer suffer from severe range limitation and have a substantial charging time which are preventing such vehicles from competing with or replacing current internal combustion engine-based vehicles. An electric motor-propelled vehicle powered by a hydrogen fuel cell for generating electricity appears to be the only functionally viable solution which has zero emissions and can yet outperform conventional vehicles in terms of driving range with a refuelling time which can be comparable to those vehicles. However, the large-scale usage of fuel cells has been stymied by their high cost coupled with insufficient infrastructure for hydrogen production and distribution, and the potential risk of carrying on-board extremely high pressure (of the order of 350-700 bar) hydrogen storage tanks in vehicles. One way to make a fuel cell stack more economical would be to optimize its design which can be achieved best by resorting to advanced Computer-Aided Engineering (CAE) techniques as implemented in a commercial multi-physics finite element analysis solver e.g. COMSOL. It is noted in this context that materials play a key role in the effective realization of a fuel cell comprising components such as gas diffusion layers, porous catalyst-coated electrodes and a solid polymer electrolyte membrane. Using the relevant physical and electro-chemical properties of the components mentioned as well as of hydrogen and oxygen, a multi-physics simulation has been carried out in the current study with the aid of COMSOL for predicting the experimental polarization curve of a single fuel cell. The single cell model is then expanded to two cells connected in parallel for scaling up the power of a fuel cell system. An approach is finally shown for arriving at the specifications of a fuel cell stack for powering an electric vehicle.

KEYWORDS: Hydrogen fuel cell; Finite element modeling; CAE; Fuel cell stack design; Electric vehicle.

https://doi.org/10.29294/IJASE.6.S2.2020.35-42

1. INTRODUCTION

Increasing use of fossil fuels as the motive energy for automobiles and other transportation systems is seriously jeopardizing human health and the eco-system on earth. The need for emission-free vehicles is driving the automotive Original Equipment Manufacturers (OEMs) to look for alternative propulsion systems such as electric motors, which can deliver high torques at low speeds – a distinct advantage compared to polluting IC engines burning fossil fuels. An obvious choice for powering a tractive electric motor is a set of batteries. However, the energy density of even the most advanced batteries is still way behind that of hydrocarbon-based fuels leading to battery-powered electric vehicles (EVs) being serioulsy handicapped in terms of driving range. Added to this is the cost of batteries based on rare-earth elements such as lithium, and the substantial time that it takes in charging batteries compared to the minutes it takes in filling up the fuel tank of a conventional vehicle. As a substitute for a battery pack as the energy source for an EV, a hydrogen-powered fuel cell holds out great promise as it can overcome the range-and charging time-related limitations of battery-powered EVs. The cost of fuel cells and the lack of infrastructure for production and distribution of hydrogen, however, remain as significant hindrances on the path of large-scale adoption of fuel cells for providing motive power to EVs.

In the present study, an estimation of specifications of a fuel cell stack required to propel a desired motor in an EV is carried out by considering the parameters of a single cell. A single high temperature PEM (Proton Exchange Membrane) fuel cell is numerically evaluated using the COMSOL multi-physics solver to predict its polarization curve. A review of literature shows that most of the work related to fuel cells is primarily limited to a single fuel cell and its constituent components such as gas diffusion layers, catalyst-coated electrodes and a solid electrolyte, as well as the electro physio-chemical processes which are involved. A few studies have dealt with specific issues such as hydrogen leakage, species transport and electrical performance of a small stack. The current study lays emphasis on the role of Computer-Aided Engineering (CAE)-driven design of a fuel cell stack keeping in mind its end use for an electric vehicle application. It is noted that CAE is an indispensable tool in modern vehicle design as it cuts down the numberof physical prototypes to a minimum, thereby significantly reducing the time and cost involved in designing a vehicle and its sub-systems. Additionally, a validated CAE procedure can be a powerful tool for design optimization such as weight reduction and

**Corresponding Author: adeb@iisc.ac.in*

Received: 11.10.2019 **Accepted:** 18.12.2019 **Published on**: 27.01.2020

performance enhancement.

Jacobson et.al. [1] stated that switching from fossil fuel to hydrogen would be a technological hurdle but also pointed out the advantages such as economic benefits and reduced dependence on depleting fossil fuels. Ahluwalia et. al. [2] envisioned hydrogen as a clean and sustainable energy for future generations that reduces the economic burden of importing fossil fuels faced bymany countries. Experimental and numerical studies on high temperature PEM fuel cell (HT-PEMFC) were performed by various researchers. Polybenzimidazole (PBI) membranes are widely used due to their favorable properties such as mechanical and chemical stability, ignition resistance, high proton conductivity, moisture regainability, improved power density, higher tolerance of anode poisoning by CO, improved chemical kinetics, and enhancement of fuel cell efficiency [3]. Savadogo [4] conducted an extensive study of alternative proton conducting membranes that operate at high temperatures and compared these with low temperature perfluorinated membranes. They concluded that the PBI–alkaline and other polymer–alkaline or organic–organic blends are promising materials for developing appropriate high temperature composite membranes for PEMFC applications. Ma et. al. [5] studied the conductivities of PBI membranes for HT-PEMFC under controlled temperature. Arsenio et. al. [6] studied proton conducting poly (2,5-benzimidazole) membranes for HT-PEMFCs and concluded that sulfuric acid doping and heat-treatment of such membranes increase acid uptake and in turn increase conductivity. Cheddie et. al. [7, 8] predicted the polarization performance of a high temperature PBI membrane fuel cell using one- and three-dimensional (3D) numerical models.Ubong, Shi and Wang [9] observed that absence of experimental data creates a gap between idealistic and realistic predictions. Hence, they developed a 3D model to evaluate the polarization curve, a key characteristic of a fuel cell,and compared the same against experimental data for a high temperature PBI-based PEM fuel cell. The model yielded good correlation with experimental results,and also provided insights into the distribution of reactants in gas diffusion layer and flow channel. Hu et. al. [10] performed an experimental and numerical study by varying the clamping load during stack assembly of a PEMFC and proposed a datum for clamping forces for real-world stack assembly. Hari et. al. [11] studied the design of a microtubular solid oxide fuel cell stack by coupling CFD and FEA models to capture the multiphysics nature of the system. However, the focus of their study was on the fluid distribution, dissipation of heat, and deformation of the fuel cell components. Sezign et. al. [12] studied the effect of inlet gas velocities and the conductivity of polymer membrane in a high temperature fuel cell using a multiphysics solver viz. COMSOL. Drakselová et. al. [13] developed a three dimensional finite element model of an industrial scale HT-PEMFC stack consisting of 100 cells for evaluation of the performance of the stack for design. The authors used COMSOL multiphysics solver for analysis. The methodology however does not provide any correlation between the performance of a single cell vis-à-vis multiple cells and also the effect of arranging cells for scaling up voltage and current density which is addressed by the work reported here by the current authors.

The finite element (FE) modelling and validation of a single cell in the current study using COMSOL by-and-large follow the procedures discussed in [9,14]. However, after obtaining satisfactory prediction of the experimental polarization curve [9] for a single cell, the same is extended to a combination of two fuel cell units configured in parallel leading to about 80% increase in current density. As expected, the voltage range for a duel cell stack with component cells connected in parallel is same as that of a single cell. Realizing that the voltage and current requirements of an EV can only be met by a stack of fuel cells connected in both series and parallel, a procedure is shown for estimating the desired array of fuel cells by taking into account the tractive requirements for a typical passenger EV.The current modeling procedure can be extended in future for analyzing an entire fuel cell stack and optimizing its performance.

2. MATERIALS AND METHODS

A hydrogen fuel cell is an electrochemical cell that converts chemical energy of hydrogen and oxygen into electrical energy through reduction and oxidation reactions. The main components of a fuel cell are flow channel, gas diffusion layer (GDL), porous electrode and electrolyte. In Fig. 1 is shown the exploded view of a HT-PEM fuel cell. The circuit potential is due to an electrochemical reaction which causes a voltage drop in the circuit and associated losses. The voltage drop is generally classified into three parts:an activation over-potential caused by the electrochemical reactions, followed by an ohmic drop across the polymer electrolyte, and mass transfer limitations of reactants [19]. At the anode, hydrogen is oxidised releasing electrons, and oxygen is reduced at the cathode. A Proton Exchange Membrane (PEM) doped with phosphoric acid only allows the protons (H^+) to pass through it. The electrons produced at the anode are carried to the cathode through the external circuit. The hydrogen protons along with electrons and the oxygen molecules combine at the cathode to produce water, and release heat by exothermic reaction. The catalyst is applied over both cathode and anode which speed up the electrochemical processes. The reactions take place on the catalysed electrode surfaces as soon as the reactants are transported by diffusion and/or convection. The relevant electrochemical reactions are depicted below:

At anode:

$$H_2 \Rightarrow 2H^+ + 2e^- \qquad (1)$$

At cathode:

$$O_2 + 4H^+ + 4e^- \Rightarrow 2H_2O \quad (2)$$

To predict the performance of a HT-PEM fuel cell, a 3D model is developed with an assumption of water exiting in vapour form since the operation of fuel cell is above 100^{0}C [16]. Also, zero water drag coefficient is assumed for flow from anode to cathode, and the gas mixture is treated as an ideal gas [9].

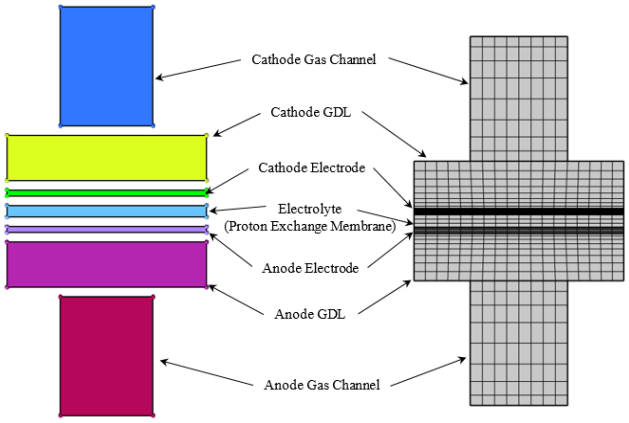

(a)

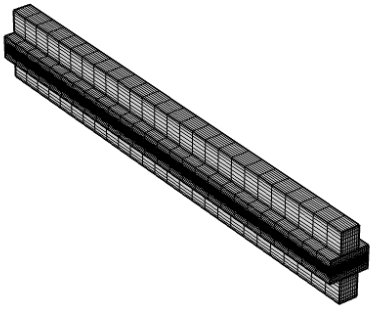

(b)

Figure 1. (a) Exploded end view and corresponding section of the FE model of an HT-PEM fuel cell; (b) Perspective view of 3D FE model

2.1 Governing Equations

Conservation of mass states that the change of mass in a unit volume must be equal to the sum of all species entering or exiting the volume in a given time period. Momentum conservation gives the net rate of change of momentum per unit volume due to convection, pressure, viscous friction and pore structure according to the following equations [9]:

$$\boldsymbol{\nabla}.(\rho \boldsymbol{u}) = 0 \quad (3)$$

$$\rho \boldsymbol{u}.\nabla \boldsymbol{u} = -\nabla p + \boldsymbol{\nabla}.[\mu(\nabla \boldsymbol{u} + (\nabla \boldsymbol{u})^T)] + \boldsymbol{\nabla}.[\lambda(\boldsymbol{\nabla}.\boldsymbol{u})\boldsymbol{I}] \quad (4)$$

where, u is the gas mixture velocity vector (m/s), ρ is the gas mixture density (kg/m^3), p is the pressure (N/m^2), μ is the dynamic viscosity of the mixture (kg/m s) and λ is the volume viscosity. It is assumed here that volume viscosity and body force are negligible, and therefore the associated terms can be ignored. These assumptions can be applied to gas channel, GDL and porous electrode. Since the flow is considered as laminar, pressure drop is proportional to gas velocity; hence the following equation holds good [9]:

$$\left(\mu/_k\right)\boldsymbol{u} = \nabla\{-p\boldsymbol{I} + \left(1/_\varepsilon\right)\mu[(\nabla \boldsymbol{u} + (\nabla \boldsymbol{u})^T)]\} \quad (5)$$

where, k is the permeability (m^2) and ε is the porosity of the GDL.

Species conservation gives the net rate of species mass change due to convection, diffusion and electrochemical reaction. Maxwell-Stefan diffusion equation [9] describes multispecies mass transports in a computation domain and solves for the fluxes of each species in terms of mass fraction. This is applied to gas channel, GDL, catalyst layer and membrane. In a PEM fuel cell, current is differentiated as ionic and electronic currents. Protons from the anode travel through the PEM membrane (ionic conductor) giving rise toan ionic current, while electrons travel through an external circuitfrom the anode to the cathode resulting in an electronic current. The conservation of electric charges or current continuity is given using the Ohm's law [9].

A constitutive equation is one that relates a cause (species) to an effect(current density) at anode and cathode. In the present context, the current density at anode and cathode can be estimated using the following simplified Bulter-Volmer Equations [9]:

$$j_a = ai_{0,a}^{ref}\left(\frac{C_{H_2}}{C_{H_2,ref}}\right)^{0.5}\left(\frac{\alpha_a+\alpha_c}{RT}F\eta_a\right) \quad (6)$$

$$j_c = ai_{0,c}^{ref}\left(\frac{C_{O_2}}{C_{O_2,ref}}\right)exp\left(-\frac{\alpha_c}{RT}F\eta_c\right) \quad (7)$$

where, $i_{0,a}^{ref}$ and $i_{0,c}^{ref}$ are the local current densities at a reference condition at anode and cathode respectively;$C_{H_2}, C_{H_2,ref}, C_{O_2}$and $C_{O_2,ref}$ are the molar concentrations of hydrogen and oxygen (mol m^{-3});α_a and α_c are the anodic and cathodic transfer coefficients for hydrogen and oxidation reactions;R is the universal gas constant (8.314 J/(mol K));T is the cell operating temperature (K); F is the Faraday constant (coulomb/mol); and η represents the potential difference.

The fuel cell model is analyzed using a commercialmulti-physics finite element code named COMSOL. The model is meshed with a total of 20,176 hexahedral elements. The values used in the current study for various model parameters are given in Table 1 and are adapted from Ubong, Shi and Wang [9]. The average inlet velocity is based on the stoichiometric ratio, active area and channel dimension [9] i.e.0.2 m/s at anode and 0.5 m/s at cathode. The flow is assumed asfully developed with flow at the outletbeing at atmospheric pressure. A symmetric boundary is assumed with no slip condition along the walls and surfaces. The anode is assumed to be grounded i.e. at 0 V;the cathode is assumed to be at the cell operating voltage of 0.9 V, and the remaining boundaries are insulated.

Table 1 Input Parameters for Simulation [9]

Operating conditions	
Humidified temperature (°C)	28
Fuel cell temperature (°C)	180
Anode inlet gas flow rate	Stoic = 1.2
Cathode inlet gas flow rate	Stoic = 2.0
Backpressure (Pa)	101325
Mass fraction of H2O_cathode	0.023 (calculated)
Mass fraction of O2 _ cathode	0.228 (calculated)
Mass fraction of H2 _ anode	0.743 (calculated)
Anode reference voltage (V)	0
Open-circuit voltage (V)	0.93
Dynamics viscosity anode at 180°C (Pa s)	1.19×10^{-5} (calculated)
Dynamics viscosity cathode at 180°C (Pa s)	2.46×10^{-5} (calculated)
Membrane properties	
Ionic conductivity, σ_m (S m^{-1})	9.825
PBI membrane thickness (μm)	100 (BASF)
GDL Properties	
Electrical conductivity, σ_d (S m^{-1})	222 (E-TEK)
Porosity	0.4
Permeability, k_p (m^2)	1.18×10^{-11}
Thickness (μm)	380 (BASF)
Gas channel dimensions	
Simulated length (cm)	2
Channel cross section (mm^2)	0.7874×1
Width of the shoulder (mm)	0.90932
Channel patterns	Serpentine
Catalyst layer information	
Catalyst layer thickness (μm)	50
Anode exchange current density (A m^{-2})	1×10^5
Cathode exchange current density (A m^{-2})	1
Binary diffusion coefficient	
$D_{O_2-N_2}$ at 293.2 K (m^2/s)	2.2×10^{-5}
$D_{O_2-H_2O}$ at 308.1 K (m^2/s)	2.82×10^{-5}
$D_{H_2O-N_2}$ at 307.5 K (m^2/s)	2.56×10^{-5}
$D_{H_2O-N_2}$ at 307.5 K (m^2/s)	2.56×10^{-5}
$D_{H_2O-N_2}$ at 307.1 K (m^2/s)	9.15×10^{-5}

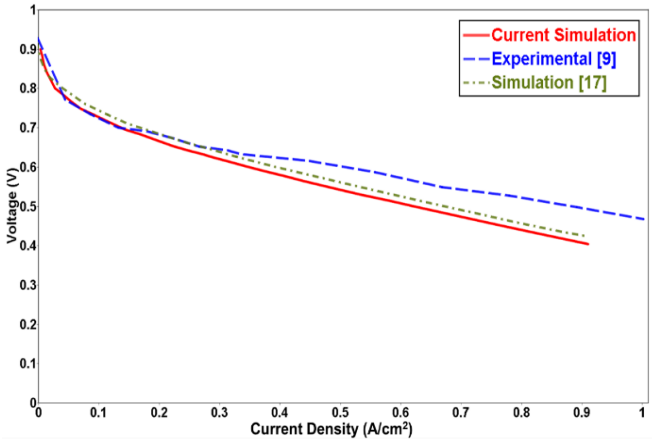

Figure 2. Polarization curves of a high temperature PEM fuel cell

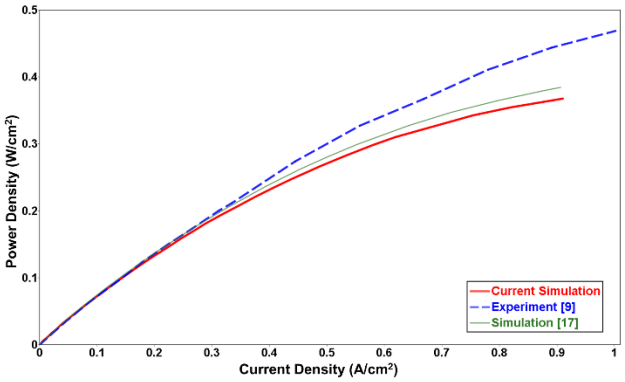

Figure 3. Power density versus current density curves of the fuel cell considered in Fig. 2

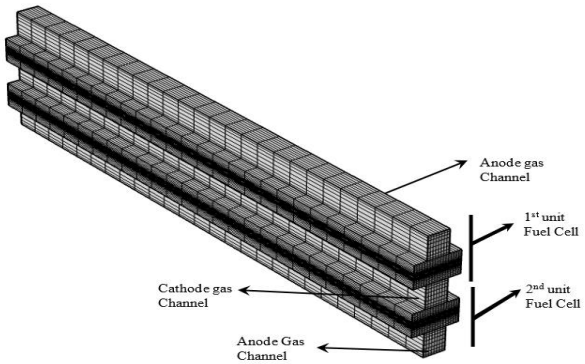

Figure 4 A FE model of a combination of two fuel cells in a parallel configuration

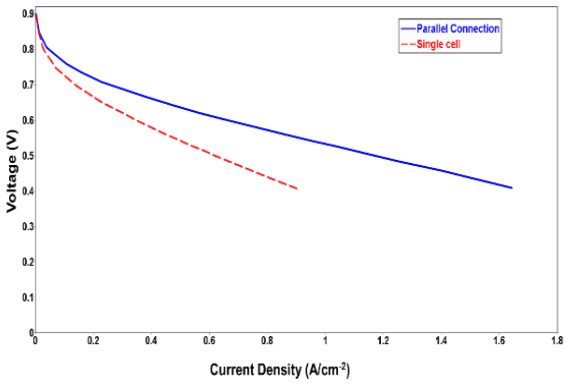

Figure 5. Voltage versus current density of a double fuel cell stack configured in parallel compared against that of a single cell

In Fig. 2 is shown the voltage versus current density behavior of the fuel cell. The simulated curve is in good agreement with the polarization curves reported [9, 10]. The power density versus current density curve obtained from the current simulation is compared against available experimental [9] and simulation [17] results in Fig. 3, and an especially good correlation is observed with the latter.

In order to achieve a desired output, a number of single fuel cellscan be combined, as if in a parallel mode, and rows of these can be connected in series to form a stack of fuel cells. In the current study, a parallel arrangement of two cells has been studied assuming that the cells are sandwiched with a common oxygen gas channel as displayed in the FE model of the combination in Fig. 4. In a parallel stacking of cells, the current density is expected to increase while maintaining the voltage level as nearly constant as can be seen in the computed result for the FE model in Fig 5.

It is noted that the values of the relevant model parameters used for the single cell in Fig. 1 are duplicated for the fuel cell stack in Fig. 4.

3. DESIGN OF A FUEL CELL STACK

Hydrogen fuel cells can have a system efficiency of upto 65% (SOFC with CHP type fuel cells) and it varies depending on the type of catalyst, membranes, type of flow and operating conditions [17]. A limited amount of literature is available on the designing of a fuel cell for electric vehicleapplications. The preliminary sizing of a fuel cell stack can be carried out through vehicle dynamics (and hence powertrain)considerations and various defining parameters of a single cell of hydrogen fuel cell. The initial estimation is based on road loadcomponentsviz. Aerodynamic drag, rolling resistance, gradient load and inertial force. The second part includes the selection of characteristic parameters such as voltage, current density and active area of thePEM inFig. 2. The parameters are chosen to suit a vehicle considered for design.

3.1 Estimation of Tractive Effort

When designing a fuel cell for powering an automobile, there are a number of forces mentioned that come into play, and the fuel cell system needs to provide enough power to overcome these forces to propel a vehicle. Additionally, for an accelerating vehicle, the inertial force i.e. forward acceleration times the mass needs to be added to the total resistive force [18]. Thus, an estimated total tractive force is

$$F_{total} = F_{aero} + F_{rr} + F_g + F_{iner} \quad (8)$$

Where,F_{aero} = aerodynamic resistance, F_{rr} = rolling resistance, F_g = gradient resistance, andF_{iner} = inertial force.

The various power components can be consolidated in terms to a total mechanical power (P_{total_mech}) required by the motion of vehicle [19, 20]

$$P_{total_{mech}} = c_1 C_d C_h A(V + V_h)^2 + \frac{C_r V(c_2 V + c_3) MgCos(\theta)}{1000} + MgVSin(\theta) + MaV \quad \text{----------(9)}$$

where in Eq. (9),$c_1$is a constant that is equal to 0.047285, C_d is vehicle drag coefficient (0.7), C_h is altitude coefficient (0.9218),A is vehicle frontal area (0.5 m^2), V is vehicle speed (30 km/h), V_h is headwind speed (3.6 km/h), C_r is coefficient of rolling resistance (1), c_2, c_3 are rolling resistance coefficients (0.0328, 4.575), M is total vehicle mass (1000 kg), g is acceleration due to gravity (9.81 m/s^2), θ is road gradient (5°), and 'a' is maximum vehicle acceleration (1.85 m/s^2).

The amount of power output can be calculated by applying the inefficiencies in the system [18]:

$$P_{vehicle\_output} = \frac{P_{total\_mech}}{\eta_{drivetrain}} + P_{auxiliary} + P_{parasitics} \quad \text{-----(10)}$$

where $P_{auxiliary}$ is the power needed by auxiliary systems, such as headlights, dashboard and other internal systems, $\eta_{drivetrain}$ is the efficiency of the electric motor and controller subsystem, and $P_{parasitics}$is the power needed by the fuel cell system, such as blowers, fans etc. [20]. For simplicity, the auxiliary and parasitic powers are considered as negligible when compared to the total mechanical power. For more accurate vehicle output power, the above factors must be estimated individually. The required motor power calculated using Eqs. (9) and (10), based on the parameters mentioned in Hesham et. al. [20] and assuming a drivetrain efficiency of 85%, is 14.45 kW. Considering the availability of motors, a BLDC (Brushless DC) motor operating at a voltage of 48 V and an average current of 200 A with a power of 20 kW is assumed.

3.2 Estimation of Fuel Cell Stack Size

In order to power an electric motor, a fuel cell system must provide sufficient voltage and current. Hence, it is necessary to arrange the fuel cell units simultaneously in series and parallel configurations. In a purely parallel configuration, currents sum up maintaining voltage as constant, while in a series arrangement, the current remains constant while voltages get added. The number of cells required in each configuration can then be estimated as follows:

$$N_{cells\_series} = \frac{Operating\ voltage}{Cell\ voltage} \quad (11)$$

$$N_{cells\_parallel} = \frac{Peak\ current}{Cell\ current} \quad (12)$$

For the targeted electric motor, using Eqs. (11) and (12), the number of cells required in series connection is obtained by dividing the motor operating voltage (48 V) by the cell voltage (0.4 V)

i.e. 120 cells; and, the number of cells required in an equivalent parallel configuration is obtained by dividing the motor peak current (200 A) with the cell current (40 A) i.e. 5. Hence, a total of (120 X 5) i.e. 600 cells in an array of series and parallel connections are required to formulate the stack.The number of cells arrived there may seem rather high but with the selection of a power train with lower peak current requirement and a fuel cell with appropriate geometric and performance characteristics, the total number of cells can be substantially reduced. It is noted that Toyota Mirai which is a commercially available hydrogen fuel cell-powered electric vehicle reportedly has a fuel cell stack consisting of 370 cells.

4. CONCLUSION

In the present study, finite element analysis of a single high temperature PEM fuel cell using the commercial COMSOL multi-physics solver has been carried out, and the predicted polarization curve is shown to correlate well with a published experimental behaviour. With an eye on formulating a methodology for a fuel cell stack design, the validated finite element modelling methodology is extended to the analysis of a two-cell stack in an equivalent parallel configuration and a consistent polarization curve is obtained in which the voltage level remained practically same as that of the single cell but the current density doubled. A preliminary design approach has then been demonstrated for estimating the specifications of a fuel cell stack for a compact electric vehicle with moderate performance. The CAE (Computer-Aided Engineering) methodology discussed can be utilized in future for optimizing the design of a fuel cell stack of a desired configuration.

REFERENCES

[1]. Jacobson, M.Z., Colella, W.G. and Golden, D.M., 2005. Cleaning the air and improving health with hydrogen fuel-cell vehicles. Science, 308(5730), 1901-1905.

[2]. Ahluwalia, R.K., Wang, X., Rousseau, A. and Kumar, R., 2004. Fuel economy of hydrogen fuel cell vehicles. Journal of Power Sources, 130(1-2), 192-201.

[3]. Ajmal Kalathil, Ajith Raghavan, Balasubramanian Kandasubramanian, 2019. Polymer Fuel Cell Based on Polybenzimidazole Membrane: A Review. Polymer-Plastics Technology and Materials, 58:5, 465-497.

[4]. Savadogo,O., 2004. Emerging membranes for electrochemical systems: Part II. High temperature composite membranes for polymer electrolyte fuel cell (PEFC) applications. Journal of Power Sources, 127(1–2), 10, 135-161.

[5]. Ma, Y.L., Wainright, J.S., Litt, M.H. and Savinell, R.F., 2004. Conductivity of PBI membranes for high-temperature polymer electrolyte fuel cells. Journal of Electrochemical Society, 151(1), A8-A16.

[6]. Asensio, J.A. and Gómez-Romero, P., 2005. Recent Developments on Proton Conduc-ting Poly (2, 5-benzimidazole) (ABPBI) Membranes for High Temperature Polymer Electrolyte Membrane Fuel Cells. Fuel Cells, 5(3), 336-343.

[7]. Cheddie, D.F. and Munroe, N.D., 2006. Three dimensional modeling of high temperature PEM fuel cells. Journal of Power Sources, 160(1), 215-223.

[8]. Cheddie, D. and Munroe, N., 2006. Mathematical model of a PEMFC using a PBI membrane. Energy Conversion and Management, 47(11-12), 1490-1504.

[9]. Ubong, E.U., Shi, Z. and Wang, X., 2009. Three-dimensional modeling and experimental study of a high temperature PBI-based PEM fuel cell. Journal of the Electrochemical Society, 156(10), B1276-B1282.

[10]. Guilin Hu, Xiaojun Wu, Yange Suo, Yuzhen Xia, Yousheng Xu, Zhiguo Zhang., 2018. Finite element analysis of PEMFC assembling based on ANSYS. International Journal of Electrochemical Science, 13, 2080 – 2089.

[11]. Hari,b., J.P. Brouwer, A. Dhir, R. Steinberger-Wilckens., 2019. A computational fluid dynamics and finite element analysis design of a microtubular solid oxide fuel cell stack for fixed wing mini unmanned aerial vehicles. International journal of hydrogen energy 44, 8519-8532.

[12]. Berna Sezgin, Dilara Gulcin Caglayan, Yilser Devrim., 2016. Modeling and sensitivity analysis of high temperature PEM fuel cells by using Comsol Multiphysics. International journal of hydrogen energy 41, 10001-10009.

[13]. Monika Drakselová, Roman Kodým, Dalimil Snita, Frank Beckmann, Karel Bouzek., 2018. Three-dimensional macrohomogeneous mathematical model of an industrial-scale high-temperature PEM fuel cell stack. Electrochimica Acta, 273, 432-446.

[14]. Mark Fowler, Mass transport analysis of a high temperature PEM fuel cell, https://www.comsol.com/blogs/pem-fuel-cell-modeling-examples/

[15]. Ionescu, V., 2014Finite element method modelling of a high temperature PEM fuel cell. Rom. Journ. Phy. 59 (3-4). 285-294.

[16]. Schmidt, T.J. and Baurmeister, J., 2008. Properties of high-temperature PEFC Celtec®-P 1000 MEAs in start/stop operation mode. Journal of Power Sources, 176(2), 428-434.

[17]. Carton, J.G. and Olabi, A.G., 2010. Design of experiment study of the parameters that affect performance of three flow plate configurations of a proton exchange membrane fuel cell. Energy, 35(7), 2796-2806.

[18]. Spiegel, C., 2007. Designing and building fuel cells (Vol. 87). New York: Mcgraw-hill.

[19]. Mahala, K.M. and Deb, A., 2011. Development of Transmission Specifications for an Electric Vehicle. In ICORD 11: Proceedings of the 3rd International Conference on Research into Design Engineering, Bangalore, India, 10.-12.01.

[20]. Hesham, R, Ivana, L, Sergio Henrique Demarchi, Jose' Reynaldo Setti., Michel Van Aerde, 2001. Vehicle Dynamics Model for Predicting Maximum Vehicle Acceleration Levels, Journal of Transportation Engineering. 127(5)

Selection and/or Peer-review under the responsibility of 2nd International Conference on Current Trends in Materials Science and Engineering, July 2019, Kolkata